Title

Glucosylsphingosine evokes pruritus via activation of 5-HT2A receptor and TRPV4 in sensory neurons

Journal

British Journal of Pharmacology, 179(10)

ISSN

0007-1188

Authors

Sanjel, Babina
Kim, Bo-Hyun
Song, Myung-Hyun
et al.

Publication Date

2022-05-01

DOI

10.1111/bph.15733

Peer reviewed

HHS Public Access

Author manuscript

Br J Pharmacol. Author manuscript; available in PMC 2022 May 17.

Published in final edited form as:

Br J Pharmacol. 2022 May ; 179(10): 2193–2207. doi:10.1111/bph.15733.

Glucosylsphingosine evokes pruritus via activation of 5-HT_{2A} receptor and TRPV4 in sensory neurons

Babina Sanjel[1,2], **Bo-Hyun Kim**[1,2], **Myung-Hyun Song**[1], **Earl Carstens**[3], **Won-Sik Shim**[1,2]

[1]College of Pharmacy, Gachon University, Incheon, South Korea

[2]Gachon Institute of Pharmaceutical Sciences, Incheon, South Korea

[3]Department of Neurobiology, Physiology and Behavior, University of California, Davis, California, USA

Abstract

Background and purpose: Glucosylsphingosine (GS), an endogenous sphingolipid, is highly accumulated in the epidermis of patients with atopic dermatitis (AD) due to abnormal ceramide metabolism. More importantly, GS can evoke scratching behaviours. However, the precise molecular mechanism by which GS induces pruritus has been elusive. Thus, the present study aimed to elucidate the molecular signalling pathway of GS, especially at the peripheral sensory neuronal levels.

Experimental approach: Calcium imaging was used to investigate the responses of HEK293T cells or mouse dorsal root ganglion (DRG) neurons to application of GS. Scratching behaviour tests were also performed with wild-type and *Trpv4* knockout mice.

Key results: GS activated DRG neurons in a manner involving both the 5-HT_{2A} receptor and TRPV4. Furthermore, GS-induced responses were significantly suppressed by various inhibitors, including ketanserin (5-HT_{2A} receptor antagonist), YM254890 (Gαq/11 inhibitor), gallein (Gβγ complex inhibitor), U73122 (phospholipase C inhibitor), bisindolylmaleimide I (PKC inhibitor) and HC067047 (TRPV4 antagonist). Moreover, DRG neurons from *Trpv4* knockout mice exhibited significantly reduced responses to GS. Additionally, GS-evoked scratching behaviours were greatly decreased by pretreatment with inhibitors of either 5-HT_{2A} receptor or TRPV4. As

Correspondence: Won-Sik Shim, College of Pharmacy, Gachon University, Incheon 21936, South Korea, wsshim@gachon.ac.kr.
Babina Sanjel and Bo-Hyun Kim have equally contributed to this work.

AUTHOR CONTRIBUTIONS

B.S. and B.-H.K. designed the research, analysed the data and drafted the manuscript; B.S., B.-H.K., and M.-H.S. performed the experiments; E.C. provided the technical support and wrote the manuscript; W.-S.S. supervised the entire research and wrote the manuscript.

CONFLICT OF INTEREST

The authors declare that there are no conflict of interest.

DECLARATION OF TRANSPARENCY AND SCIENTIFIC RIGOUR

This declaration acknowledges that this paper adheres to the principles for transparent reporting and scientific rigour of preclinical research as stated in the BJP guidelines for Design and Analysis, Immunoblotting and Immunochemistry, and Animal Experimentation and as recommended by funding agencies, publishers and other organizations engaged with supporting research.

SUPPORTING INFORMATION

Additional supporting information may be found in the online version of the article at the publisher's website.

expected, GS-evoked scratching behaviour was also significantly decreased in *Trpv4* knockout mice.

Conclusion and implications: Overall, the present study provides evidence for a novel molecular signalling pathway for GS-evoked pruritus, which utilizes both 5-HT_{2A} receptor and TRPV4 in mouse sensory neurons. Considering the high accumulation of GS in the epidermis of patients with AD, GS could be another pruritogen in patients with AD.

Keywords

5-HT_{2A} receptor; atopic dermatitis; glucosylsphingosine; pruritus; TRPV4

1 | INTRODUCTION

Itch, or pruritus, is an unpleasant, irritating sensation that evokes a desire to scratch. Typically, itch signals are initiated by the triggering action of pruritogens (itch-inducing compounds), which excite peripheral sensory neurons that innervate the skin. These itch-inducing signals are mediated by various receptors and ion channels (Dong & Dong, 2018).

Pruritus hampers the quality of normal daily life, especially when it becomes chronic (Akiyama & Carstens, 2014). Chronic pruritus, defined as continuous pruritus that lasts for more than 6 weeks (Stander et al., 2007), is often associated with dermatological diseases, such as atopic dermatitis (AD). Indeed, chronic pruritus is a hallmark clinical feature of AD (Stander, 2021).

Pruritus in AD is mediated by various pruritogens. Intriguingly, histamine is not a major pruritogen in AD (Stander, 2021). Instead, roles for non-histamine pruritogens such as IL-4, IL-13, IL-31 and thymic stromal lymphopoietin (TSLP) have been elucidated in AD (Cevikbas et al., 2014; Oh et al., 2013; Wilson et al., 2013). Still, there may be as yet unexplored pruritogens and/or molecular pathways responsible for pruritus in AD.

In this context, the present study aimed to verify whether glucosylsphingosine (GS), an endogenous sphingolipid, could act as a putative pruritogen in AD, since GS is highly accumulated in the skin of patients with AD (Imokawa, 2021; Ishibashi et al., 2003) (detailed explanation can be found in the Supplementary information). Importantly, GS evokes itch-related scratching responses in mice (Kim et al., 2010). Furthermore, we have previously found that GS activates the heterologously expressed 5-HT_{2A} receptor (Afzal & Shim, 2017).

Serotonin (5-hydroxytryptamine or 5-HT) is an inflammatory mediator that can evoke itch (Kushnir-Sukhov et al., 2007; Slominski et al., 2003). Indeed, intradermal injection of serotonin elicits robust scratching behaviour in rodents (Nojima & Carstens, 2003; Yamaguchi et al., 1999). Additionally, application of serotonin in humans elicits mild to moderate itch (Hosogi et al., 2006; Kushnir-Sukhov et al., 2007; Weisshaar et al., 1997, 2004). Moreover, aberrant serotonin signalling in the skin is linked to itch in patients with AD (Huang et al., 2004; Soga et al., 2007).

Transient receptor potential vanilloid subtype 4 (TRPV4) is a non-selective cationic ion channel expressed in sensory neurons that sense various chemical, mechanical and thermal stimuli (White et al., 2016). Interestingly, TRPV4 is involved in serotonin-induced pruritus via 5-HT_2 receptor in mice (Akiyama et al., 2016). Indeed, TRPV4 antagonists substantially reduced the serotonin-induced scratching in mice (Akiyama et al., 2016). Since GS can activate 5-HT_{2A} receptor (Afzal & Shim, 2017), it is anticipated that GS-evoked pruritus may be mediated through 5-HT_{2A} receptor and/or TRPV4.

Therefore, we aimed to elucidate the detailed molecular mechanisms underlying GS-induced pruritus in sensory neurons. Specifically, we examined whether GS triggers pruritus through the activation of 5-HT_{2A} receptor and/or TRPV4 in peripheral sensory neurons in mice.

2 | METHODS

2.1 | Materials

Glucosylsphingosine (CAS# 52050-17-6; also known as glucosyl[β] sphingosine [d18:1] or D-glucosyl-β1-1-D-erythro-sphingosine), ketanserin, HC067047, U73122, gallein and bisindolylmaleimide I (BIM I) were purchased from Sigma-Aldrich (Incheon, South Korea). YM254890 was purchased from Weko (Osaka, Japan).

2.2 | Genes

Mouse 5-HT_{2A} receptor (*Htr2A*), human *TRPV1*, mouse *Trpv3*, mouse *Trpm3*, human *TRPA1* and human *TRPV4* cDNAs were subcloned into the pcDNA3.1 (Invitrogen) vector. Additionally, *TRPV4* cDNA was also subcloned into pIRES-EFGP (Invitrogen), allowing TRPV4 and EGFP to be translated from a single bicistronic mRNA, and further used in whole-cell patch-clamp experiments. All genes showed 100% identity with the genes deposited in the NCBI GenBank database. For measurement of cAMP, a gene that encodes a synthetic fluorescent peptide called ‘Pink flamindo’ (Kazuki Harada et al., 2017) was used. Pink Flamindo was a gift from Tetsuya Kitaguchi (Addgene plasmid #102356; RRID:Addgene_102356).

2.3 | Cell culture and transfection

HEK293T cells were cultured in Dulbecco’s modified Eagle’s medium (DMEM) containing 10% heat-inactivated foetal bovine serum (FBS) and 1% penicillin. To transiently express the genes of interest, cells were transfected with FuGENE®HD Transfection reagent (Promega, Madison, WI, USA) according to the manufacturer’s instructions. Briefly, cDNAs were transfected with 2:1 ratio (reagent: cDNA), and calcium imaging was performed 24 h after the transfection.

2.4 | Animals

Animal studies are reported in compliance with the ARRIVE guidelines (Percie du Sert et al., 2020) and with the recommendations made by the *British Journal of Pharmacology* (Lilley et al., 2020). All experimental animal protocols were approved by the Institutional Animal Care and Use Committee of Gachon University (GIACUC-R2020002) and were performed in accordance with the guidelines for the Care and Use of Laboratory Animals.

Nine-week-old male ICR mice were purchased from Koatech (Pyeongtaek, Gyeonggi-do, Korea). The principle of 3Rs (Replacement, Refinement and Reduction of Animals) were taken into consideration for the sample sizes of animal experiments, using randomization and blinded analysis (Curtis, Ashton et al., 2018). Only male mice were used in the present study since female mice seem to scratch more than males (Green et al., 2006; Liu et al., 2012).

For *Trpv4* knockout mice (*Trpv4* KO), breeding pairs of heterozygous B6.129X1-Trpv4<tm1Msz> were purchased from RIKEN (Wako, Saitama Prefecture, Japan, RRID:SCR_001065) (Mizuno et al., 2003; Suzuki et al., 2003). Homozygous *Trpv4* KO offspring were verified by genomic typing using the PCR protocol provided by RIKEN. All *Trpv4* KO mice showed a homogeneous deletion of TRPV4. Six-to-ten-week old male homozygous *Trpv4* KO mice were used in the study, and no noticeable behavioural changes were observed during the experiment.

2.5 | Scratching behaviour test

The experiment was initially designed to include balanced group sizes. However, due to some unexpected mistakes and errors (e.g., incomplete injection of compound and skin injuries found before experiment), the group size varied in some conditions. The compounds were dissolved in saline and injected intradermally into the nape (50 μl) or the cheek (10 μl) of the mice. Alternatively, mice were pretreated intraperitoneally with the compounds 30 min before the nape injection. For comparison, either 5-HT_{2A} receptor antagonist (ketanserin) or TRPV4 antagonist (HC067047) was intraperitoneally administered to mice 30 min before GS injection. Scratching behaviour was video-recorded for up to 30 min. By reviewing the recorded video, the scratching bouts of the animals were counted by experienced researchers in a blinded manner. One bout of scratching was defined as the movement of hind limb scratching near the injected area until it touched the floor.

2.6 | Primary culture of mouse DRG neurons

DRG neurons were primarily cultured as described previously (Sanjel et al., 2019). Briefly, mouse DRG neurons were collected and incubated for 60 min at 37°C with 1 mg/ml collagenase (Worthington Biochemical, Lakewood, NJ, USA), followed by an additional 40 min incubation with 2.5 mg/ml trypsin (Gibco, Gangnam, Korea). After 10 min of centrifugation at 30×g, cells were dissolved in neurobasal medium containing 10% heat-inactivated FBS, 5 ng/ml nerve growth factor (NGF; Invitrogen, Gaithersburg, MD, USA) and 100 U/ml ZellShield® (Minerva BioLabs, Berlin, Germany) and plated on a poly L-lysine-treated eight-well chamber (Lab-Tek, Naperville, IL, USA). Then, the cells were incubated for 2 days in 95% humidity and 5% CO_2 at 37°C. DRG neurons were prepared from two mice per one experiment, and three independent experiments were conducted for the calcium imaging.

2.7 | Calcium imaging

Intracellular calcium levels were determined by calcium-specific fluorescent dye (Fluo-3/AM) using fluorescence microscopes (ECLIPSE Ti-U; Nikon, Tokyo, Japan and Leica DMi8 inverted microscope; Leica Microsystems Ltd., Wetzlar, Germany). Fluo-3/AM

(5 μM; Invitrogen, Carlsbad, CA, USA), and 0.1% F127 mixtures were loaded into the cells for 40 min at 37°C. After 40 min, supernatants were removed and washed with 1 × NBS (normal buffer solution: 140 mM NaCl, 5 mM KCl, 2 mM $CaCl_2$/EDTA, 0.5 mM $MgCl_2$, 10 mM glucose and 5.5 mM HEPES, adjusted to pH 7.4). The excitation wavelength was 488 nm, and the emitted fluorescence was measured at 515 nm. After treatment with the compounds, changes in the fluorescent images were recorded. Ca^{2+} influx was expressed as the F/F_0 ratio, where Findicates the fluorescence intensity of the cell or region of interest (ROI) while F_0 indicates the initial fluorescence intensity. Image analysis was completed with ImageJ (NIH, RRID:SCR_003070) with custom scripts for semiautomatic ROI count, F/F_0 ratio calculation and image production. It should be emphasized that ROIs in microscopic images were *not* manually selected by researchers since this may cause bias. Instead, we used ImageJ for unbiased computer-assisted ROI recognition. This process resulted in approximately 1,000 to 2,000 total ROIs per group when all ROIs from three independent experiments (six separate wells) were combined. Since drawing scatter plots with more than 1,000 values was not possible in GraphPad Prism, we had to reduce the number by choosing only 10% of the total ROIs. To achieve this, we used the 'random selection' function in Kutools for Excel (ExtendOffice.com) to randomly choose 10% of ROI. It was confirmed that the 10% randomly selected ROIs are not different from the total ROIs since there was no difference of the average and distribution profile between the two groups. This process finally resulted in around 100 to 200 ROIs per group, allowing scatter plots to be drawn in GraphPad Prism. Since each F/F_0 value represents a time course profile of separate cells, these individual values are not technical replicates. Group size refers to the total number of cells selected to calculate the F/F_0 ratio. To calculate the percentage of GS-responsive cells, the criterion "$F/F_0 > 2$" was used.

2.8 | Immunohistochemistry

DRG sections were cut using a cryostat (20 μm thick) and attached to the slides. The tissue sections were washed with phosphate-buffered saline (PBS) and fixed with 4% paraformaldehyde for 10 min. Hydrogen peroxide (1%) was used to suppress endogenous peroxidase activity, and 0.3% Triton X-100 with 1% FBS was used for blocking. The samples were then incubated overnight at 4°C with TRPV4 rabbit polyclonal antibody (Abcam, ab39260, RRID:AB_1143677) at 1:200 dilution and HTR2A goat polyclonal antibody (Abcam, ab140824) at 1:200 dilution. The next day, the samples were washed with PBS and incubated with goat anti-rabbit IgG H&L secondary antibody (Alexa Fluor® 488; Abcam, ab150077, RRID:AB_2630365) at 1:1,000 dilution and donkey anti-goat IgG H&L secondary antibody (Alexa Fluor® 647; Abcam, ab150131, RRID:AB_2732857) at 1:1,000 dilution for 2 h in the dark to avoid photobleaching. Primary and secondary antibodies were prepared in 0.3% Triton-X 100 containing 0.5% FBS. After washing the samples with PBS, freshly prepared DAPI staining solution in PBS was added, and the samples were incubated for 10 min in the dark. The samples were rinsed two to three times with PBS, mounted with VECTASHIELD® (Vector Laboratories, Burlingame, CA, USA) and covered with a coverslip. The slides were visualized, and images were obtained using a Leica DMi8 inverted microscope (Leica Microsystem Ltd., Wetzlar, Germany). The immuno-related procedures used comply with the recommendations made by the *British Journal of Pharmacology* (Alexander et al., 2018).

2.9 | Whole-cell voltage-clamp recording

HEK293T cells cultured in DMEM with 10% heat-inactivated FBS and 1% ZellShield® were seeded appropriately in T75 flasks to achieve 60–80% confluency on the day of the experiment. The day after the seeding, cells were transfected using FuGENE®HD reagent with TRPV4 cDNA that was subcloned into the pIRES-eGFP vector (pIRESeFGP-TRPV4), so that the expression of TRPV4 can be verified by eGFP fluorescence. Twenty-four hours after transfection, eGFP fluorescence was detected after transfection of pIRES-eFGP-TRPV4 (data not shown). With these cells, whole-cell voltage-clamp experiments were conducted using Nanion Port-a-Patch (Nanion Technologies GmbH, Munich, Germany) following the recommended protocol. Briefly, cells were harvested in 500 µl of external recording solution and resuspended regularly with a 1 ml pipette during experiments. The holding potential of the whole-cell configuration was set at −80 mV. For all experiments, NPC-1© chips (Nanion Technologies GmbH, Munich, Germany) were used. Data were acquired using HEKA software and analysed using Stimfit (Guzman et al., 2014).

2.10 | Data presentation and statistical analysis

All the data and statistical analyses comply with the recommendations of the *British Journal of Pharmacology* on experimental design and analysis in pharmacology (Curtis, Alexander, et al., 2018). Data were presented as the mean ± 95% confidence interval (CI). Statistical tests were performed using GraphPad Prism software (version 9, RRID: SCR_002798). As the data from the calcium imaging did not show the homogeneity of the variances, nonparametric comparisons in Figures 1f, 2d, 3b,d,f,h, 4c,d, and 5b,c were made either by Mann–Whitney test (between two groups) or by nonparametric Kruskal–Wallis test followed by Dunn's test (among more than three groups). Other data, such as peak currents (Figure 4h) and behaviour tests (Figure 6), showed a normal distribution and homogeneity of the variances. Comparisons in these cases were made using the unpaired student's *t* test (two groups) or one-way analysis of variance (ANOVA) followed by Dunnett's post hoc tests. In the case of Figure 2b, Fisher's exact test was used to compare the percentage of DRG neurons positive for the 5-HT_{2A} receptor between wild-type and *Trpv4* KO mice. Only one statistical significance threshold ($P < 0.05$) was used in all analyses.

2.11 | Nomenclature of targets and ligands

Key protein targets and ligands in this article are hyperlinked to corresponding entries in http://www.guidetopharmacology.org and are permanently archived in the Concise Guide to PHARMACOLOGY 2021/22 (Alexander et al., 2021).

3 | RESULTS

3.1 | GS activates sensory neurons through 5-HT_{2A} receptor and TRPV4

We first examined whether or not GS can induce changes in peripheral sensory neurons. To this end, we made a primary culture of mouse DRG neurons and performed calcium imaging experiments to test the effect of GS. When 100 µM GS was applied, an increase in intracellular calcium levels was observed (Figure 1a, $n = 92$ cells). Among the total analysed cells, 34 cells (37%) were responsive to GS. Treatment with a high concentration

of KCl (100 mM) also evoked an increase in intracellular calcium levels, implying that the responding cells were neurons (Figure 1a,d). When GS was reapplied 5 min after the first GS treatment, the second GS application also evoked an increase in intracellular calcium levels (Figure S1). However, the response to the second GS was not different from that of the first GS.

We next investigated whether the response is mediated by 5-HT_{2A} receptor. This is based on the previous report that GS can activate 5-HT_{2A} receptor when transiently expressed in HEK293T cells (Afzal & Shim, 2017). Thus, ketanserin ('Ket'), an antagonist of 5-HT_{2A} receptor, was applied before GS treatment. The response to GS application was significantly decreased by pretreatment with 10 μM ketanserin (Figure 1b, n = 174 cells), while 15 cells (8.6%) were still responsive to GS. Thus, it suggests that GS-induced responses are mediated in part by 5-HT_{2A} receptor in the mouse sensory neurons.

It was previously reported that serotonin-evoked scratching in mice requires both the serotonin receptor (ketanserin-sensitive) and TRPV4 ion channel (Akiyama et al., 2016; Snyder et al., 2016). Thus, we further examined if the GS-induced response is also mediated through TRPV4. Similar to ketanserin, 10 μM HC067047 ('HC', a specific TRPV4 antagonist) was applied before GS application. HC067047 pretreatment indeed suppressed the GS response (Figure 1c, n = 154 cells), while 22 cells (14.3%) still showed responses to GS. These results suggest that GS may also activate TRPV4. Moreover, pretreatment of both ketanserin and HC067047 ('HC + Ket') also strongly reduced the effect of GS (Figure 1d–f n = 159 cells), and only five cells (3.1%) were responsive to GS.

Therefore, these data clearly indicate that GS can activate mouse sensory neurons through 5-HT_{2A} receptor and TRPV4.

3.2 | GS-induced responses are attenuated in DRG neurons of Trpv4 KO mice

Because both 5-HT_{2A} receptor and TRPV4 are involved in the GS-induced excitation of DRG, we investigated whether the two molecules are co-expressed by the same DRG population. As shown in Figure 2a (top row), both 5-HT_{2A} receptor and TRPV4 were expressed in the wild-type DRG sections, whereas only 5-HT_{2A} receptor was expressed in those from *Trpv4* KO mice (bottom row). Among total 560 wild-type cells, 44 cells showed co-expression of both 5-HT_{2A} receptor and TRPV4 (Figure 2b, left), implying that a putative intracellular interaction between the two could be possible. In total 377 *Trpv4* KO cells, 86 cells were positive to 5-HT_{2A} receptor, and TRPV4 expression was not found at all (Figure 2b, middle). In addition, the percentages of 5-HT_{2A} receptor-positive cells were not significantly different between wild-type and *Trpv4* KO mice (Figure 2b, right-hand graph; Fisher's exact test). This validates the use of *Trpv4* KO mice.

To further investigate the role of TRPV4 in GS-induced responses, calcium imaging experiments were performed using DRG neurons from both wild-type and *Trpv4* KO mice. As shown in Figure 2c,d, responses to 100 μM GS were significantly lower in DRG neurons from *Trpv4* KO (n = 130 cells; 19.2% [25 cells] showed responses), when compared to those from wild-type mice (n = 111 cells; 39.6% [44 cells] showed responses). Moreover, 10 and 100 μM GS treatment also showed reduced maximum F/F_0 values in cells from

Trpv4 KO compared to wild types, while there was no difference in responses to the lowest concentration of GS (1 μM) (Figure 2d). Thus, these data demonstrate the involvement of TRPV4 for GS-evoked responses in mouse DRG neurons.

3.3 | GS utilizes both Gαq/11- and Gβγ-mediated signalling pathways in mouse DRG neurons

To investigate the downstream signalling pathway(s) of the GS-induced response, mouse DRG neurons were pretreated with various inhibitors that can block specific molecules prior to the application of 100 μM GS. Since 5-HT_{2A} receptor is a GPCR linked to Gαq/11 (Filip & Bader, 2009), we first tested if pretreatment with YM254890 (a Gαq/11 inhibitor) affected the rise in GS-induced intracellular calcium levels. We found that 10 μM YM254890 suppressed the intracellular calcium increase (n = 93 cells) when compared to the control (n = 121 cells), suggesting that Gαq/11 mediates GS-induced responses (Figure 3a,b). Furthermore, we examined whether the remaining Gβγ complex was involved in the GS-induced response in DRG neurons. To verify this, 10 μM gallein (a Gβγ complex inhibitor) was pretreated similarly, which resulted in significantly decreased responses (n = 130 cells; Figure 3a, b). The effect of gallein was found to be stronger than YM254890 (Figure 3b). Moreover, 10 μM co-pretreatment of YM254890 and 10 μM gallein strongly inhibited GS-induced responses (n = 108 cells; Figure 3a,b). Therefore, it was concluded that GS utilizes both Gαq/11 and to a greater extent Gβγ complex for activation of its downstream signalling pathway in mouse DRG neurons.

We further investigated if GS-induced responses involve Gαi/o and/or Gαs. As shown in Figure 3c,d, pretreatment of 250 ng/ml PTX (a Gαi/o inhibitor) in DRG neurons did not alter GS-induced responses (n = 130 cells) when compared to control (n = 85 cells), suggesting that GS-induced responses do not take advantage of Gαi/o. Furthermore, measurement of cAMP in HEK293T cells expressing 5-HT_{2A} receptor revealed that GS treatment did not induce any cAMP production, implying that Gαs is unlikely to be involved (Figure S2A). Thus, it is suggested that GS is unlikely to utilize Gαi/o and/or Gαs for its activation mechanism.

Because activation of Gαq/11 subunit and Gβγ complex commonly leads to stimulation of phospholipase C (PLC) (Philip et al., 2010; Smrcka & Sternweis, 1993), we investigated the effect of pretreatment with U73122 (a PLC inhibitor) on GS-induced DRG activation. As a result, it was found that 10 μM U73122 successfully inhibited the increase in intracellular calcium induced by GS (n = 130 cells) when compared to control (n = 126 cells), indicating that PLC activation mediates GS-induced responses in mouse DRG neurons (Figure 3e,f).

PLC activation catalyses the breakdown of phosphatidylinositol 4,5-bisphosphate (PIP_2) into inositol triphosphate (IP_3) and diacylglycerol (DAG), which can further activate protein kinase C (PKC). Interestingly, there are reports that TRPV4 activation is sensitized when PKC is activated (Mercado et al., 2014; Peng et al., 2010). For these reasons, we tested the effect of pretreatment with 10 nM BIM I (a PKC inhibitor) in mouse DRG neurons and found that GS-induced activation was significantly decreased (n = 142 cells) when compared to control (n = 92 cells) as well (Figure 3g,h). Decisively, the increase in calcium increase in mouse DRG neurons was completely eliminated when a calcium-free buffer was

used (Figure S2B), suggesting that the source of calcium is exclusively extracellular, not intracellular calcium store.

Overall, these data have revealed downstream mechanisms of the GS-induced signalling pathway in mouse DRG neurons. Specifically, it is found that GS-induced actions are mediated by Gαq/11 and Gβγ complex, which in turn activates downstream enzymes such as PLC and PKC to evoke calcium influx in mouse sensory neurons.

3.4 | GS can directly activate TRPV4

At this point, we have assumed that the GS-induced response is initiated by 5-HT_{2A} receptor, which in turn activates downstream enzymes, leading to the opening of TRPV4 as a final step. Thus, we initially hypothesized that GS-induced TRPV4 activation mandates 5-HT_{2A} receptor expression. To test this idea, HEK293T cells were transiently transfected with *TRPV4*, and the effect of GS was measured by calcium imaging.

HEK293T cells transfected with a mock vector ('pcDNA') showed virtually no response to 100 μM GS (Figure 4a). To our surprise, however, the application of 100 μM GS to HEK293T cells expressing TRPV4 elicited a significant increase in intracellular calcium even in the absence of 5-HT_{2A} receptor (Figure 4b). Therefore, these data strongly imply that the GS-induced responses can be mediated solely by TRPV4. Furthermore, the GS-evoked responses showed dose-dependency (Figure 4c). Most importantly, GS-induced responses were significantly inhibited when pretreated with a selective TRPV4 inhibitor, HC067047 (Figure 4d). Thus, it was assumed that TRPV4 is independently responsive to GS.

Then, it was examined whether other TRP channels can be activated by GS. TRP channels previously known to be involved in itch sensation were transiently expressed in HEK293T cells. Transfected cells were stimulated with 50 μM GS in calcium imaging experiments. As shown in Figures 4e and S3, GS was found to activate TRPV4 more strongly (n = 188 cells) than other TRP channels, showing that TRPV4 is the most sensitive TRP channel to GS.

To further confirm whether GS can directly activate TRPV4, whole-cell patch-clamp experiments were performed. When 100 μM GS was applied in control cells transfected with the mock vector, GS failed to induce inward currents (Figure 4f). However, robust inward currents were observed in cells transfected with *TRPV4* after GS treatment (Figure 4g), implying that GS-induced inward currents are mediated by TRPV4. As shown in Figure 4h, the average peak currents induced by GS significantly increased in TRPV4-expressing cells (Control: 15.80 ± 5.920 pA vs. TRPV4: 428.9 ± 63.70 pA, n = 6/group). Therefore, these data clearly revealed that GS can directly activate TRPV4, as opposed to the initial hypothesis that GS may require 5-HT_{2A} receptor to activate TRPV4.

3.5 | GS induces the strongest responses when both 5-HT_{2A} receptor and TRPV4 are coexpressed

It was further tested whether GS can synergistically activate cells expressing both 5-HT_{2A} receptor and TRPV4. Three different groups of HEK293T cells that transiently express 5-HT_{2A} receptor (5-HT_{2A}), TRPV4 or both 5-HT_{2A} and TRPV4 ('5-HT_{2A} + TRPV4') were

prepared. All three groups showed evident responses to 25 μM GS (Figure 5a,b). In detail, the two groups expressing either 5-HT_{2A} or TRPV4 alone showed similar responses to GS. However, the '5-HT_{2A} + TRPV4' group showed the most robust GS-induced responses. Thus, it was confirmed that cells that express both 5-HT_{2A} receptor and TRPV4 can exhibit the strongest responses to GS application.

Furthermore, it was examined whether '5-HT_{2A} + TRPV4' group can mimic signalling pathways verified in DRG neurons. For this reason, identical downstream inhibitors used in Figure 3 were similarly applied to '5-HT_{2A} + TRPV4'. Similar to data in Figure 3, each of the inhibitors significantly suppressed the responses to GS (Figure 5c), supporting the validity of data obtained from '5-HT_{2A} + TRPV4' in HEK293T cells.

In summary, these data imply that maximal GS-induced responses can be obtained in cells that express both 5-HT_{2A} receptor and TRPV4.

3.6 | GS evokes scratching behaviour via 5-HT_{2A} receptor and TRPV4 in mouse

To investigate whether GS can evoke scratching behaviours via 5-HT_{2A} receptor and TRPV4, we initially injected GS (250 nmol per site) intradermally into the cheek because the cheek model can distinguish whether the compound is inducing itch (scratching) or pain (wiping) (Shimada & LaMotte, 2008). As shown in Figure 6a, the cheek injection of GS evoked increased scratching bouts (63.71 ± 18.05, $n = 7$) than the vehicle-injected control group (21.43 ± 5.843, $n = 7$), suggesting that GS is indeed a pruritogen. Furthermore, there was no difference in wiping behaviour between the two groups (Figure S4A).

It was further verified if GS-induced scratching is mediated by 5-HT_{2A} receptor and TRPV4. As shown in Figure 6b, GS injection into the nape also evoked significantly increased scratching bouts (92.17 ± 24.32, $n = 6$), when compared to the control group ('Veh'; vehicle injection, 20.50 ± 6.920, $n = 8$). More importantly, the number of scratching bouts was significantly reduced when mice were pretreated with either 3 mg/kg ketanserin (1.000 ± 0.6814, $n = 8$) or 10 mg/kg HC067047 (26.73 ± 6.409, $n = 11$) (Figure 6a). Therefore, it was concluded that GS-evoked scratching behaviour is mediated by both 5-HT_{2A} receptor and TRPV4 in mice.

In addition, we expanded the GS-induced behaviour experiments to *Trpv4* KO mice. It was first confirmed that *Trpv4* KO mice exhibited normal scratching behaviours toward chloroquine, a different type of pruritogen that activates MRGPRA3 irrelevant to TRPV4. As shown in Figure S4B, the data suggest that the scratching behaviours are not disturbed in *Trpv4* KO mice.

GS was then intradermally injected into the nape of wild-type or Trpv4 KO mice. As shown in Figure 6c, wild-type mice scratched 101.1 ± 21.14 bouts ($n = 7$) after GS injection, while bouts of scratching in *Trpv4* KO mice were significantly lower (41.83 ± 6.258 bouts, $n = 6$). When the scratching bouts were further divided into 5 min intervals (Figure 6d), most GS-induced scratching behaviour started from 5 min after the injection.

In general, the mouse behaviour study has revealed that GS evokes scratching behaviour via 5-HT_{2A} receptor and TRPV4.

4 | DISCUSSION

The present study has expanded our understanding of GS functions; GS is not just a disrupted-skin-barrier marker but also a functional sphingolipid that can elicit pruritus. As mentioned earlier, GS can evoke scratching behaviours when injected into mice (Kim et al., 2010), and we also obtained the same data (Figure 6). Considering the high accumulation of GS in the epidermis of AD, GS can be regarded as a novel AD-specific pruritogen. However, the precise molecular mechanism(s) underlying the GS-induced pruritus has not been revealed until the present study. The only indication was that the GS-induced scratching behaviours were attenuated by cycloheptadine (a 5-HT_2 receptor inhibitor) but not by ketotifen (an H1-antagonist) (Kim et al., 2010). These results implicate the involvement of serotonin receptors in the GS-induced signalling pathway, but not histamine receptors. Although we have previously revealed that GS can activate mouse 5-HT_{2A} receptor (Afzal & Shim, 2017), the data were not sufficient because GS-induced activity was only verified in the reconstituted cell line. In this context, it should be noted that the present study has finally revealed a molecular signalling pathway for GS-induced pruritus, especially at the peripheral sensory neuronal levels.

The present study discovered new underlying mechanisms related to the GS-induced signalling pathways. First, we showed that 5-HT_{2A} receptor plays an essential role in GS-induced pruritus in peripheral sensory neurons. DRG neurons are known to express various subtypes of serotonin receptors (Ohta et al., 2006), but 5-HT_{2A} and 5-HT_7 receptors are potentially involved in various instances of acute and chronic pruritus. For example, HTR7 was reported to mediate serotonin-evoked itch via TRPA1 in mice (Morita et al., 2015). Additionally, acute serotonin-evoked scratching behaviour is mediated by 5-HT_2 receptors in rodents (Akiyama et al., 2016; Nojima & Carstens, 2003). Because of the importance of 5-HT_2 and 5-HT_7 receptors in various itch conditions, we cannot rule out the possibility that 5-HT_7 receptor might also be involved in GS-evoked pruritus. In fact, there is a report that ketanserin can also inhibit 5-HT_7 receptor (Plassat et al., 1993), implying a plausible involvement of 5-HT_7 receptor in the GS-induced pruritus. However, an earlier study has reported that 5-HT_7 receptor is mainly linked to Gαs and causes calcium level increase from the intracellular calcium store (Baker et al., 1998). Importantly, GS-induced calcium responses were disappeared in the calcium-free buffer (Figure S2B), suggesting that the GS-induced calcium level increase was not derived from the intracellular calcium store. Thus, it is expected that the involvement of the 5-HT_7 receptor in GS-induced pruritus would be minimal, if any. Nevertheless, further investigation is required to clarify the relationship between GS and 5-HT_7 receptor in the future.

Another novel finding deduced from the present study is the involvement of TRPV4 in GS-evoked pruritus. TRPV4 is a member of the TRP channel family, which is involved in the transmission of various stimuli, such as temperature, pain and itch, in the peripheral sensory neurons (Moore et al., 2018). For example, TRPV1 is a channel required for the transmission of histamine-dependent itch pathways (Shim et al., 2007). Likewise, TRPA1 is another TRP channel involved in distinct histamine-independent pruritus (Kittaka & Tominaga, 2017). TRPV4 is also an important channel for pruritus via TRPV1-mediated facilitation (Kim et al., 2016). Similarly, a recent report also claimed the importance of

TRPV4 in cinnamaldehyde-evoked scratching in mice (Domocos et al., 2020). Besides, TRPV4-expressing macrophages and keratinocytes contribute to chronic itch (Luo et al., 2018), and TRPV4 is upregulated in skins with post-burn itching conditions (Moore et al., 2013; Yang et al., 2015). Considering these broad roles of TRPV4 in pruritus, it is not surprising that TRPV4 also mediates GS-induced pruritus.

Another interesting fact revealed in the present study is that there is a functional link between the 5-HT_{2A} receptor and TRPV4. However, this coordinated activation mode between the serotonin receptor and TRPV4 is not entirely new. In fact, it was originally reported that serotonin induces itch sensation via the serotonin receptor and TRPV4 in mouse sensory neurons (Akiyama et al., 2016). It was also found that *Trpv4* KO mice showed significantly decreased scratching bouts to serotonin, implying a potential link between the serotonin receptor and TRPV4. Based on this study, we have assumed that GS may utilize the same 5-HT_{2A} receptor and TRPV4 molecular pathway to transmit pruritus.

The so-called GPCR-TRP axis is present in sensory neurons for the translation of various stimuli into electrical signals (Veldhuis et al., 2015). Generally, a stimulant first binds to the specific GPCR, which subsequently activates certain downstream molecules, resulting in the opening of a TRP ion channel at the end. To demonstrate that GS-induced pruritus is also mediated by the GPCR-TRP axis, the intermediate molecular pathways between the 5-HT_{2A} receptor and TRPV4 must be identified. Remarkably, results from DRG primary culture (Figure 3) and HEK293T cells expressing both 5-HT_{2A} receptor and TRPV4 (Figure 5) suggest a possible involvement of PLC and PKC in the GS-induced signalling pathway.

Interestingly, it was found that PLC activation is achieved by stimulation of both Gαq/11 and Gβγ complex from the 5-HT_{2A} receptor (Figures 3a,b and 5c). Previous reports have found that Gαq/11 strongly activates PLCβ1 and PLCβ3 (Philip et al., 2010; Smrcka & Sternweis, 1993), while Gβγ complex favourably stimulates PLCβ2 and PLCβ3 (Rebres et al., 2011; Smrcka & Sternweis, 1993). Based on these findings, we predict that PLCβ3 might be a major subtype of PLC in the GS-induced signalling pathway because both the Gαq/11 and Gβγ complexes can commonly activate PLCβ3. Importantly, the involvement of PLC activation in the GS-induced signalling pathway is confirmed by pretreatment with a PLC inhibitor (U73122), which significantly inhibited the GS-induced responses (Figures 3e,f and 5c). Therefore, it is apparent that GS-induced stimulation of the 5-HT_{2A} receptor will lead to PLC activation.

Because PLC activation can further stimulate PKC in the presence of intracellular calcium, it is suggested that PKC could be involved in the GS-induced signalling pathway as well. Indeed, GS-induced responses were significantly inhibited by BIM I (Figures 3g,h and 5c), strongly supporting the role of PKC in the pathway. Although PKC can phosphorylate not only TRPV4 but other TRP channels as well (Yao et al., 2005), it is likely that TRPV4 will be the most affected by PKC because TRPV4 showed the most potent responses to GS among other TRP channels (Figure 4e). This is in agreement with the previous reports that PKC activation sensitizes TRPV4 activity (Mercado et al., 2014; Peng et al., 2010).

In summary, it is clear that (1) *GS activates 5-HT$_{2A}$ receptor with subsequent stimulation of PLC and thereby PKC to sensitize TRPV4*. Furthermore, it is also confirmed that (2) *GS can directly activate TRPV4 without 5-HT$_{2A}$ receptor*. Therefore, by combining these two observations, we propose a novel molecular signalling pathway for GS-induced pruritus in mouse sensory neurons. As summarized in Figure 7, GS can activate 5-HT$_{2A}$ receptor (5-HT$_{2A}$) with subsequent stimulation of PLC via Gαq/11 and Gβγ complex. This, in turn, will break down PIP_2 into IP_3 and DAG, which can further activate PKC to sensitize TRPV4. On the other hand, activation of the sensitized TRPV4 is directly facilitated by GS. If activation of TRPV4 is sufficient to induce depolarization, an action potential will be produced in the peripheral sensory neurons. The action potential signal will be further transmitted through the spinal cord to the brain, eventually perceived as pruritus.

However, the present study was limited in several ways. First, there might be a potential variability in itch perception between two different mouse strains (ICR and C57BL/6). For example, scratching behaviours have been reported to be quite different between various strains (Inagaki et al., 2001). Because our data were acquired from both ICR and C57BL/6 mice, there is a chance that unexpected difference might have occurred in the data. Another limitation could be that the current findings may not apply to female since only male mice were used in the experiments. It was by experimental design to reduce a factor that may complicate the interpretation, since female mice seem to scratch more than males (Green et al., 2006; Liu et al., 2012). Future studies are mandatory to examine whether there is a sex difference in terms of GS-induced itch sensation.

In conclusion, the present study provides evidence for a novel molecular signalling pathway for GS-evoked pruritus, which utilizes both 5-HT$_{2A}$ receptor and TRPV4 in sensory neurons. As GS is highly accumulated in the epidermis of patients with AD, the current findings may shed light on attempts to unravel the secrecies of intractable pruritus in patients with AD.

Supplementary Material

Refer to Web version on PubMed Central for supplementary material.

ACKNOWLEDGEMENTS

This work was supported by the National Research Foundation of Korea (NRF) grant funded by the Korea government (MSIT) (No. 2021R1A2C1005865). We would like to thank Mirela Iodi Carstens and Amanda Nguyen for their technical assistance with the *Trpv4* KO mouse scratching behaviour experiments.

Funding information

National Research Foundation of Korea, Grant/Award Number: 2021R1A2C1005865

DATA AVAILABILITY STATEMENT

The data that support the findings of this study are available from the corresponding author upon reasonable request.

Abbreviations:

AD	atopic dermatitis
BIM I	Bisindolylmaleimide
GS	glucosylsphingosine
HC	HC067047
TRPA1	Transient receptor potential ankyrin subtype 1
TRPM3	Transient receptor potential melastatin subtype 3
TRPV1/3/4	Transient receptor potential vanilloid subtype 1/3/4

REFERENCES

Afzal R, & Shim WS (2017). Glucosylsphingosine activates serotonin receptor 2a and 2b: Implication of a novel itch signaling pathway. Biomolecules & Therapeutics, 25(5), 497–503. 10.4062/biomolther.2016.207 [PubMed: 28208011]

Akiyama T, & Carstens E (2014). Spinal coding of itch and pain. In Carstens E & Akiyama T (Eds.), Itch: Mechanisms and treatment. CRC Press.

Akiyama T, Ivanov M, Nagamine M, Davoodi A, Carstens MI, Ikoma A, Cevikbas F, Kempkes C, Buddenkotte J, Steinhoff M, & Carstens E (2016). Involvement of TRPV4 in serotonin-evoked scratching. The Journal of Investigative Dermatology, 136(1), 154–160. 10.1038/JID.2015.388 [PubMed: 26763435]

Alexander SP, Kelly E, Mathie A, Peters JA, Veale EL, Armstrong JF, Faccenda E, Harding SD, Pawson AJ, Southan C, Buneman OP, Cidlowski JA, Christopoulos A, Davenport AP, Fabbro D, Spedding M, Striessnig J, Davies JA, Ahlers-Dannen KE, … Zolghadri Y (2021). THE CONCISE GUIDE TO PHARMACOLOGY 2021/22: Introduction and Other Protein Targets. British Journal of Pharmacology, 178(suppl 1), S1–S26. 10.1111/bph.15537 [PubMed: 34529830]

Alexander SPH, Roberts RE, Broughton BRS, Sobey CG, George CH, Stanford SC, Cirino G, Docherty JR, Giembycz MA, Hoyer D, Insel PA, Izzo AA, Ji Y, MacEwan DJ, Mangum J, Wonnacott S, & Ahluwalia A (2018). Goals and practicalities of immunoblotting and immunohistochemistry: A guide for submission to the British Journal of Pharmacology. British Journal of Pharmacology, 175, 407–411. [PubMed: 29350411]

Baker LP, Nielsen MD, Impey S, Metcalf MA, Poser SW, Chan G, Obrietan K, Hamblin MW, & Storm DR (1998). Stimulation of type 1 and type 8 Ca2+/calmodulin-sensitive adenylyl cyclases by the Gs-coupled 5-hydroxytryptamine subtype 5-HT7A receptor. The Journal of Biological Chemistry, 273(28), 17469–17476. 10.1074/jbc.273.28.17469 [PubMed: 9651336]

Cevikbas F, Wang X, Akiyama T, Kempkes C, Savinko T, Antal A, Kukova G, Buhl T, Ikoma A, Buddenkotte J, Soumelis V, Feld M, Alenius H, Dillon SR, Carstens E, Homey B, Basbaum A, & Steinhoff M (2014). A sensory neuron-expressed IL-31 receptor mediates T helper cell-dependent itch: Involvement of TRPV1 and TRPA1. The Journal of Allergy and Clinical Immunology, 133(2), 448–460. 10.1016/j.jaci.2013.10.048 [PubMed: 24373353]

Curtis MJ, Alexander S, Cirino G, Docherty JR, George CH, Giembycz MA, Hoyer D, Insel PA, Izzo AA, Ji Y, MacEwan DJ, Sobey CG, Stanford SC, Teixeira MM, Wonnacott S, & Ahluwalia A (2018). Experimental design and analysis and their reporting II: Uupdated and simplified guidance for authors and peer reviewers. British Journal of Pharmacology, 175, 987–993. 10.1111/bph.14153 [PubMed: 29520785]

Curtis MJ, Ashton JC, Moon LDF, & Ahluwalia A (2018). Clarification of the basis for the selection of requirements for publication in the British Journal of Pharmacology. British Journal of Pharmacology, 175(18), 3633–3635. 10.1111/bph.14443 [PubMed: 30144042]

Domocos D, Follansbee T, Nguyen A, Nguyen T, Carstens MI, & Carstens E (2020). Cinnamaldehyde elicits itch behavior via TRPV1 and TRPV4 but not TRPA1. Itch, 5(3), e36. 10.1097/itx.0000000000000036 [PubMed: 34458578]

Dong X, & Dong X (2018). Peripheral and central mechanisms of itch. Neuron, 98(3), 482–494. 10.1016/j.neuron.2018.03.023 [PubMed: 29723501]

Filip M, & Bader M (2009). Overview on 5-HT receptors and their role in physiology and pathology of the central nervous system. Pharmacological Reports, 61(5), 761–777. 10.1016/s1734-1140(09)70132-x [PubMed: 19903999]

Green AD, Young KK, Lehto SG, Smith SB, & Mogil JS (2006). Influence of genotype, dose and sex on pruritogen-induced scratching behavior in the mouse. Pain, 124(1–2), 50–58. 10.1016/j.pain.2006.03.023 [PubMed: 16697529]

Guzman SJ, Schlogl A, & Schmidt-Hieber C (2014). Stimfit: Quantifying electrophysiological data with Python. Frontiers in Neuroinformatics, 8, 16. 10.3389/fninf.2014.00016 [PubMed: 24600389]

Hosogi M, Schmelz M, Miyachi Y, & Ikoma A (2006). Bradykinin is a potent pruritogen in atopic dermatitis: A switch from pain to itch. Pain, 126(1–3), 16–23. 10.1016/j.pain.2006.06.003 [PubMed: 16842920]

Huang J, Li G, Xiang J, Yin D, & Chi R (2004). Immunohistochemical study of serotonin in lesions of psoriasis. International Journal of Dermatology, 43(6), 408–411. 10.1111/j.1365-4632.2004.02195.x [PubMed: 15186219]

Imokawa G (2021). Cutting edge of the pathogenesis of atopic dermatitis: Sphingomyelin deacylase, the enzyme involved in its ceramide deficiency, plays a pivotal role. International Journal of Molecular Sciences, 22(4), 1613. 10.3390/ijms22041613 [PubMed: 33562655]

Inagaki N, Nagao M, Igeta K, Kawasaki H, Kim JF, & Nagai H (2001). Scratching behavior in various strains of mice. Skin Pharmacology and Physiology, 14(2), 87–96. 10.1159/000056338

Ishibashi M, Arikawa J, Okamoto R, Kawashima M, Takagi Y, Ohguchi K, & Imokawa G (2003). Abnormal expression of the novel epidermal enzyme, glucosylceramide deacylase, and the accumulation of its enzymatic reaction product, glucosylsphingosine, in the skin of patients with atopic dermatitis. Laboratory Investigation, 83(3), 397–408. 10.1097/01.LAB.0000059931.66821.92 [PubMed: 12649340]

Kazuki Harada MI, Wang X, Tanaka M, Wongso D, Konno A, Hirai H, Hirase H, Tsuboi T, & Kitaguchi T (2017). Red fluorescent protein-based cAMP indicator applicable to optogenetics and in vivo imaging. Scientific Reports, 7, 7351. 10.1038/s41598-017-07820-6 [PubMed: 28779099]

Kim HJ, Kim KM, Noh M, Yoo HJ, & Lee CH (2010). Glucosylsphingosine induces itch-scratch responses in mice. Biomolecules & Therapeutics, 18(3), 316–320. 10.4062/biomolther.2010.18.3.316

Kim S, Barry DM, Liu XY, Yin S, Munanairi A, Meng QT, Cheng W, Mo P, Wan L, Liu SB, Ratnayake K, Zhao ZQ, Gautam N, Zheng J, Karunarathne WK, & Chen ZF (2016). Facilitation of TRPV4 by TRPV1 is required for itch transmission in some sensory neuron populations. Science Signaling, 9(437), ra71. 10.1126/scisignal.aaf1047 [PubMed: 27436359]

Kittaka H, & Tominaga M (2017). The molecular and cellular mechanisms of itch and the involvement of TRP channels in the peripheral sensory nervous system and skin. Allergology International, 66(1), 22–30. 10.1016/j.alit.2016.10.003 [PubMed: 28012781]

Kushnir-Sukhov NM, Brown JM, Wu Y, Kirshenbaum A, & Metcalfe DD (2007). Human mast cells are capable of serotonin synthesis and release. The Journal of Allergy and Clinical Immunology, 119(2), 498–499. 10.1016/j.jaci.2006.09.003 [PubMed: 17291861]

Lilley E, Stanford SC, Kendall DE, Alexander SP, Cirino G, Docherty JR, George CH, Insel PA, Izzo AA, Ji Y, Panettieri RA, Sobey CG, Stefanska B, Stephens G, Teixeira M, & Ahluwalia A (2020). ARRIVE 2.0 and the British Journal of Pharmacology: Updated guidance for 2020. British Journal of Pharmacology, 177(16), 3611–3616. 10.1111/bph.15178 [PubMed: 32662875]

Liu C, Liang L, Han Y, Zhang M, Xie Y, Han W, Hu S, Zhang H, & Xu H (2012). Sex differences in scratching behaviors induced by intradermal injections of pruritogenic chemicals in C57BL/6 mice. Neuroscience & Medicine, 3(3), 314–320. 10.4236/nm.2012.33036

Luo J, Feng J, Yu G, Yang P, Mack MR, Du J, Yu W, Qian A, Zhang Y, Liu S, Yin S, Xu A, Cheng J, Liu Q, O'Neil RG, Xia Y, Ma L, Carlton SM, Kim BS, … Hu H (2018). Transient receptor

potential vanilloid 4-expressing macrophages and keratinocytes contribute differentially to allergic and nonallergic chronic itch. The Journal of Allergy and Clinical Immunology, 141(2), 608–619 e7. 10.1016/j.jaci.2017.05.051 [PubMed: 28807414]

Mercado J, Baylie R, Navedo MF, Yuan C, Scott JD, Nelson MT, Brayden JE, & Santana LF (2014). Local control of TRPV4 channels by AKAP150-targeted PKC in arterial smooth muscle. The Journal of General Physiology, 143(5), 559–575. 10.1085/jgp.201311050 [PubMed: 24778429]

Mizuno A, Matsumoto N, Imai M, & Suzuki M (2003). Impaired osmotic sensation in mice lacking TRPV4. American Journal of Physiology. Cell Physiology, 285(1), C96–C101. 10.1152/ajpcell.00559.2002 [PubMed: 12777254]

Moore C, Cevikbas F, Pasolli HA, Chen Y, Kong W, Kempkes C, Parekh P, Lee SH, Kontchou NA, Yeh I, Jokerst NM, Fuchs E, Steinhoff M, & Liedtke WB (2013). UVB radiation generates sunburn pain and affects skin by activating epidermal TRPV4 ion channels and triggering endothelin-1 signaling. Proceedings of the National Academy of Sciences of the United States of America, 110(34), E3225–E3234. 10.1073/pnas.1312933110 [PubMed: 23929777]

Moore C, Gupta R, Jordt SE, Chen Y, & Liedtke WB (2018). Regulation of pain and itch by TRP channels. Neuroscience Bulletin, 34(1), 120–142. 10.1007/s12264-017-0200-8 [PubMed: 29282613]

Morita T, McClain SP, Batia LM, Pellegrino M, Wilson SR, Kienzler MA, Lyman K, Olsen AS, Wong JF, Stucky CL, Brem RB, & Bautista DM (2015). HTR7 mediates serotonergic acute and chronic itch. Neuron, 87(1), 124–138. 10.1016/j.neuron.2015.05.044 [PubMed: 26074006]

Nojima H, & Carstens E (2003). 5-Hydroxytryptamine (5-HT)2 receptor involvement in acute 5-HT-evoked scratching but not in allergic pruritus induced by dinitrofluorobenzene in rats. The Journal of Pharmacology and Experimental Therapeutics, 306(1), 245–252. 10.1124/jpet.103.049239 [PubMed: 12682216]

Oh MH, Oh SY, Lu J, Lou H, Myers AC, Zhu Z, & Zheng T (2013). TRPA1-dependent pruritus in IL-13-induced chronic atopic dermatitis. Journal of Immunology, 191(11), 5371–5382. 10.4049/jimmunol.1300300

Ohta T, Ikemi Y, Murakami M, Imagawa T, Otsuguro K, & Ito S (2006). Potentiation of transient receptor potential V1 functions by the activation of metabotropic 5-HT receptors in rat primary sensory neurons. The Journal of Physiology, 576(Pt 3), 809–822. 10.1113/jphysiol.2006.112250 [PubMed: 16901936]

Peng H, Lewandrowski U, Muller B, Sickmann A, Walz G, & Wegierski T (2010). Identification of a protein kinase C-dependent phosphorylation site involved in sensitization of TRPV4 channel. Biochemical and Biophysical Research Communications, 391(4), 1721–1725. 10.1016/j.bbrc.2009.12.140 [PubMed: 20043876]

Percie du Sert N, Hurst V, Ahluwalia A, Alam S, Avey MT, Baker M, Browne WJ, Clark A, Cuthill IC, Dirnagl U, Emerson M, Garner P, Holgate ST, Howells DW, Karp NA, Lazic SE, Lidster K, MacCallum CJ, Macleod M, … Würbel H (2020). The ARRIVE guidelines 2.0: updated guidelines for reporting animal research. PLoS Biology, 18(7), e3000410. 10.1371/journal.pbio.3000410 [PubMed: 32663219]

Philip F, Kadamur G, Silos RG, Woodson J, & Ross EM (2010). Synergistic activation of phospholipase C-beta3 by Galpha(q) and Gbetagamma describes a simple two-state coincidence detector. Current Biology, 20(15), 1327–1335. 10.1016/j.cub.2010.06.013 [PubMed: 20579885]

Plassat JL, Amlaiky N, & Hen R (1993). Molecular cloning of a mammalian serotonin receptor that activates adenylate cyclase. Molecular Pharmacology, 44(2), 229–236. [PubMed: 8394987]

Rebres RA, Roach TI, Fraser ID, Philip F, Moon C, Lin KM, Liu J, Santat L, Cheadle L, Ross EM, Simon MI, & Seaman WE (2011). Synergistic Ca2+ responses by Gαi- and Gαq-coupled Gprotein-coupled receptors require a single PLCβ isoform that is sensitive to both Gβγ and Gαq. The Journal of Biological Chemistry, 286(2), 942–951. 10.1074/jbc.M110.198200 [PubMed: 21036901]

Sanjel B, Maeng HJ, & Shim WS (2019). BAM8–22 and its receptor MRGPRX1 may attribute to cholestatic pruritus. Scientific Reports, 9(1), 10888. 10.1038/s41598-019-47267-5 [PubMed: 31350433]

Shim WS, Tak MH, Lee MH, Kim M, Kim M, Koo JY, Lee CH, Kim M, & Oh U (2007). TRPV1 mediates histamine-induced itching via the activation of phospholipase A2 and 12-lipoxygenase.

The Journal of Neuroscience, 27(9), 2331–2337. 10.1523/JNEUROSCI.4643-06.2007 [PubMed: 17329430]

Shimada SG, & LaMotte RH (2008). Behavioral differentiation between itch and pain in mouse. Pain, 139(3), 681–687. 10.1016/j.pain.2008.08.002 [PubMed: 18789837]

Slominski A, Pisarchik A, Zbytek B, Tobin DJ, Kauser S, & Wortsman J (2003). Functional activity of serotoninergic and melatoninergic systems expressed in the skin. Journal of Cellular Physiology, 196(1), 144–153. 10.1002/jcp.10287 [PubMed: 12767050]

Smrcka AV, & Sternweis PC (1993). Regulation of purified subtypes of phosphatidylinositol-specific phospholipase C beta by G protein alpha and beta gamma subunits. The Journal of Biological Chemistry, 268(13), 9667–9674. h10.1016/S0021-9258(18)98401-2 [PubMed: 8387502]

Snyder LM, Kuzirian MS, & Ross SE (2016). An unexpected role for TRPV4 in serotonin-mediated itch. The Journal of Investigative Dermatology, 136(1), 7–9. 10.1016/j.jid.2015.11.010 [PubMed: 26763416]

Soga F, Katoh N, Inoue T, & Kishimoto S (2007). Serotonin activates human monocytes and prevents apoptosis. The Journal of Investigative Dermatology, 127(8), 1947–1955. 10.1038/sj.jid.5700824 [PubMed: 17429435]

Stander S (2021). Atopic dermatitis. The New England Journal of Medicine, 384(12), 1136–1143. 10.1056/NEJMra2023911 [PubMed: 33761208]

Stander S, Weisshaar E, Mettang T, Szepietowski JC, Carstens E, Ikoma A, Bergasa NV, Gieler U, Misery L, Wallengren J, Darsow U, Streit M, Metze D, Luger TA, Greaves MW, Schmelz M, Yosipovitch G, & Bernhard JD (2007). Clinical classification of itch: A position paper of the international forum for the study of itch. Acta Dermato-Venereologica, 87(4), 291–294. 10.2340/00015555-0305 [PubMed: 17598029]

Suzuki M, Mizuno A, Kodaira K, & Imai M (2003). Impaired pressure sensation in mice lacking TRPV4. The Journal of Biological Chemistry, 278(25), 22664–22668. 10.1074/jbc.M302561200 [PubMed: 12692122]

Veldhuis NA, Poole DP, Grace M, McIntyre P, & Bunnett NW (2015). The G protein-coupled receptor-transient receptor potential channel axis: Molecular insights for targeting disorders of sensation and inflammation. Pharmacological Reviews, 67(1), 36–73. 10.1124/pr.114.009555 [PubMed: 25361914]

Weisshaar E, Dunker N, Rohl FW, & Gollnick H (2004). Antipruritic effects of two different 5-HT3 receptor antagonists and an antihistamine in haemodialysis patients. Experimental Dermatology, 13(5), 298–304. 10.1111/j.0906-6705.2004.00184.x [PubMed: 15140020]

Weisshaar E, Ziethen B, & Gollnick H (1997). Can a serotonin type 3 (5-HT3) receptor antagonist reduce experimentally-induced itch? Inflammation Research, 46(10), 412–416. 10.1007/s000110050213 [PubMed: 9372314]

White JP, Cibelli M, Urban L, Nilius B, McGeown JG, & Nagy I (2016). TRPV4: Molecular conductor of a diverse orchestra. Physiological Reviews, 96(3), 911–973. 10.1152/physrev.00016.2015 [PubMed: 27252279]

Wilson SR, The L, Batia LM, Beattie K, Katibah GE, McClain SP, Pellegrino M, Estandian DM, & Bautista DM (2013). The epithelial cell-derived atopic dermatitis cytokine TSLP activates neurons to induce itch. Cell, 155(2), 285–295. 10.1016/j.cell.2013.08.057 [PubMed: 24094650]

Yamaguchi T, Nagasawa T, Satoh M, & Kuraishi Y (1999). Itch-associated response induced by intradermal serotonin through 5-HT2 receptors in mice. Neuroscience Research, 35(2), 77–83. 10.1016/s0168-0102(99)00070-x [PubMed: 10616911]

Yang YS, Cho SI, Choi MG, Choi YH, Kwak IS, Park CW, & Kim HO (2015). Increased expression of three types of transient receptor potential channels (TRPA1, TRPV4 and TRPV3) in burn scars with post-burn pruritus. Acta Dermato-Venereologica, 95(1), 20–24. 10.2340/00015555-1858 [PubMed: 24695993]

Yao X, Kwan HY, & Huang Y (2005). Regulation of TRP channels by phosphorylation. Neurosignals, 14(6), 273–280. 10.1159/000093042 [PubMed: 16772730]

What is already known

- GS is highly accumulated in the epidermis of patients with AD.
- GS can evoke scratching behaviour.

What does this study adds

- GS-induced pruritus is mediated by 5-HT receptor and TRPV4 in peripheral sensory neurons.

What is the clinical significance

- GS can be a pruritogen in patients with AD.
- 5-HT_{2A} receptor and TRPV4 represent novel targets for inhibition of pruritus in AD.

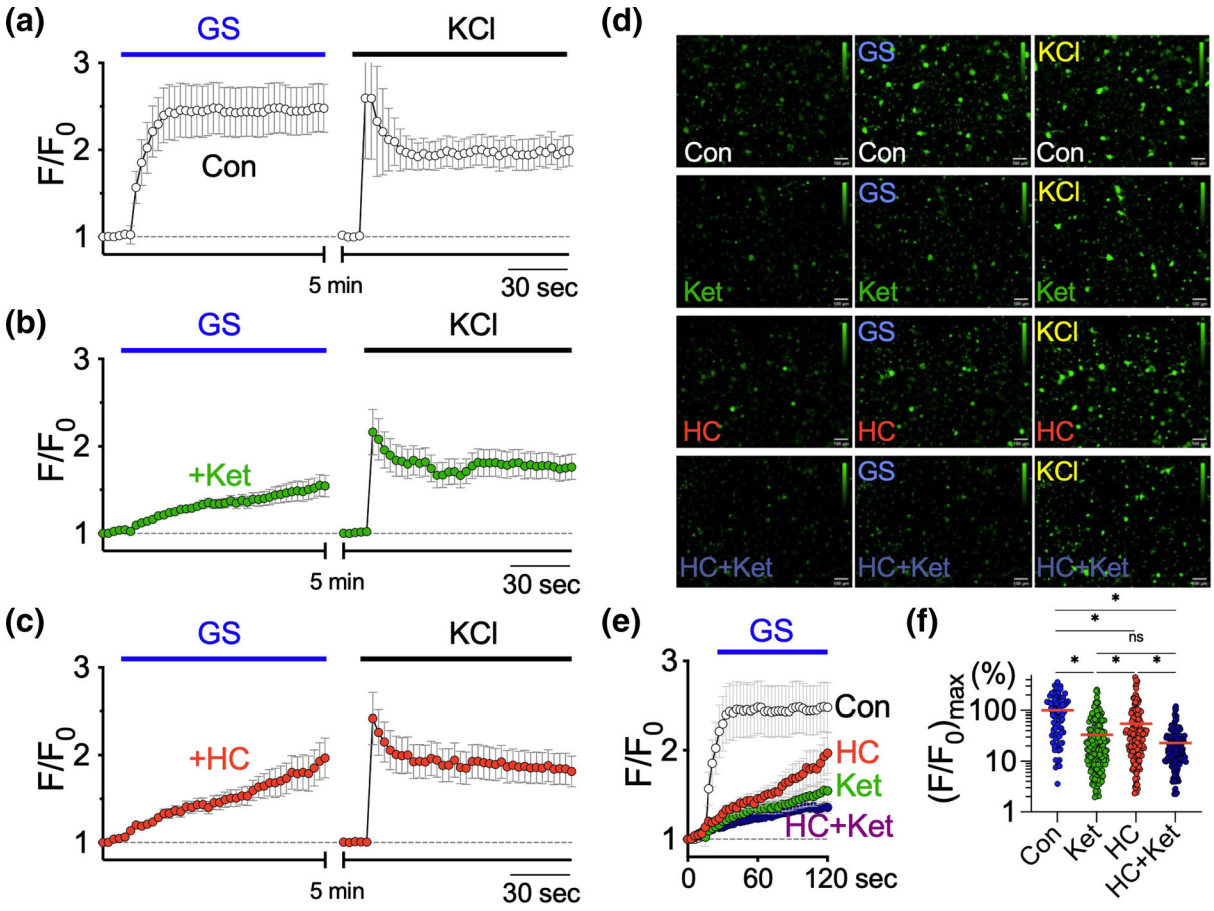

FIGURE 1.

Glucosylsphingosine (GS) induces intracellular calcium influx in mouse sensory neurons via 5-HT_{2A} receptor and TRPV4. (a) Application of 100 μM GS induced an increase in intracellular calcium in mouse sensory neurons (n = 92 cells). The empty circles with the black line represent the averaged F/F_0 values of all cells analysed. Five minutes after the GS treatment, a high concentration of KCl (100 mM) was applied. (b) Pretreatment with 10 μM ketanserin ('Ket', an antagonist of 5-HT_{2A} receptor) significantly inhibited the GS response (n = 174 cells). Green circles with the black line represent the averaged F/F_0 values of all cells analysed. (c) Pretreatment with 10 μM HC067047 ('HC', a specific TRPV4 antagonist) also suppressed the GS response (n = 154 cells). Red circles with the black line represent the averaged F/F_0 values of all cells analysed. (d) Representative fluorescent images of four different groups are shown: 'Con' (first row); control group, 'Ket' (second row); Ket-treated group, 'HC' (third row); HC-treated group, 'HC + Ket' (fourth row); both 10 μM HC- and 10 μM Ket-treated group (n = 159 cells). The left column represents the status before GS treatment. The middle columnrepresents the cellular responses after 100 μM GS application. The right column represents responses to 100 mM KCl treatment. Scale bar represents 100 μm. (e) Summarized graph of the maximal GS responses ($[F/F_0]_{max}$) from four different groups. (f) Comparison of relative maximum responses ($[F/F_0]_{max}$) among four different groups. The highest averaged value of the control group is set to 100%, and other values

were normalized. Red horizontal bar indicates the average value of each group. *$P < 0.05$; ns, not significant

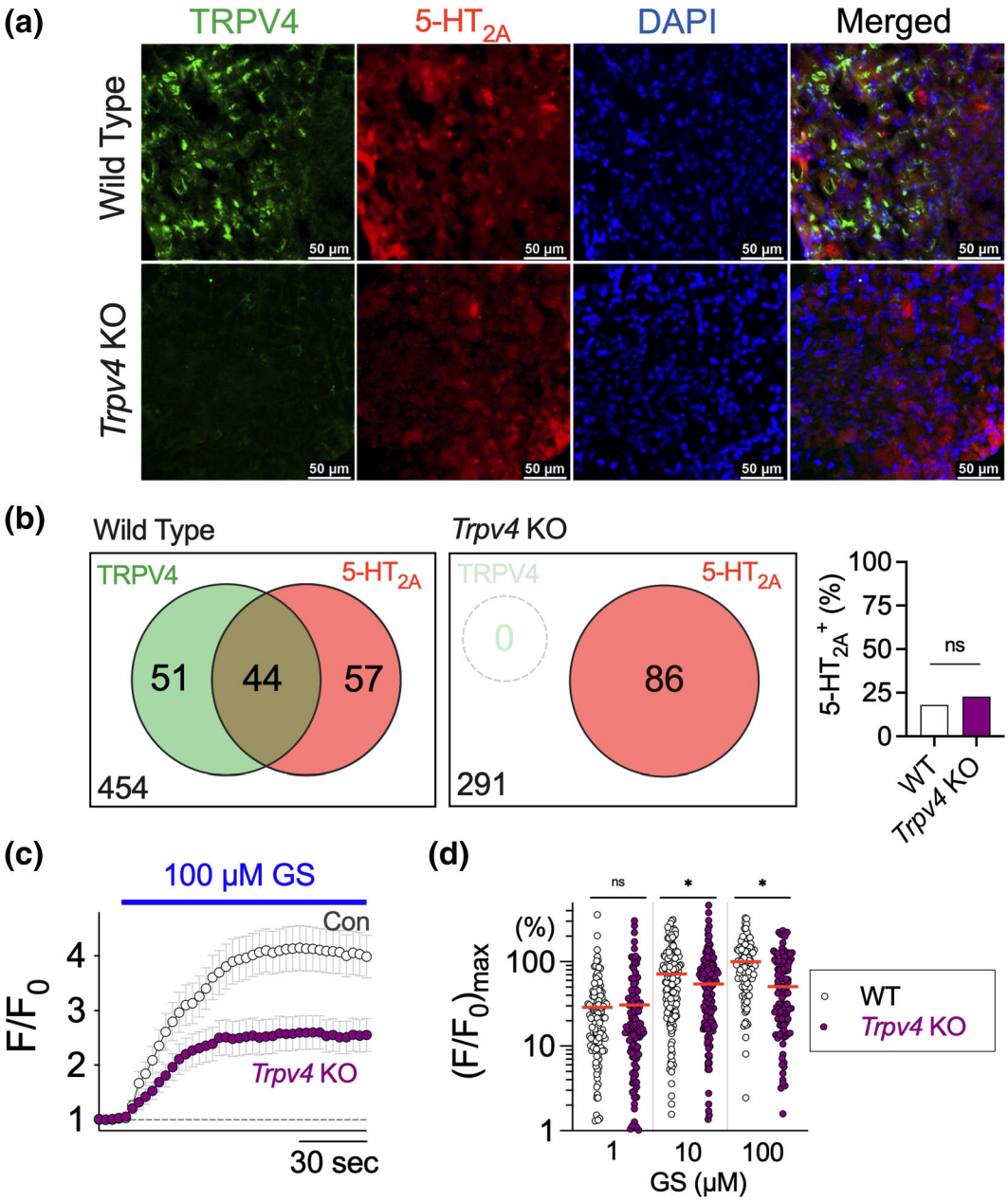

FIGURE 2.

DRG from *Trpv4* knockout (KO) mice exhibit attenuated responses to GS. (a) Representative images of immunofluorescence staining with 5-HT_{2A} receptor (5-HT_{2A})- and TRPV4-antibody in the dorsal root ganglia (DRG) of wild type (WT) and *Trpv4* KO mice. (b) Venn diagrams showing numbers of DRG in wild type (left, total 560 cells) and *Trpv4* KO (middle, total 377 cells). Fisher's exact test did not show differences in the percentages of 5-HT_{2A}-positive DRG between wild type and Trpv4 KO mice (right, $P > 0.05$). (c) The increase in intracellular calcium induced by GS was significantly reduced in *Trpv4* KO DRG cultures ($n = 130$ cells) compared to WT ($n = 111$ cells). (d) Comparison of the maximum responses to GS treatments (1, 10 and 100 µM) between WT (1 µM: $n = 142$ cells, 10 µM: $n = 171$ cells, 100 µM: $n = 111$ cells) and *Trpv4* KO mice (1 µM: $n = 125$ cells, 10 µM: n

= 169 cells, 100 μM: n = 130 cells). Red horizontal bar indicates the average value of each group. *P < 0.05; ns, not significant

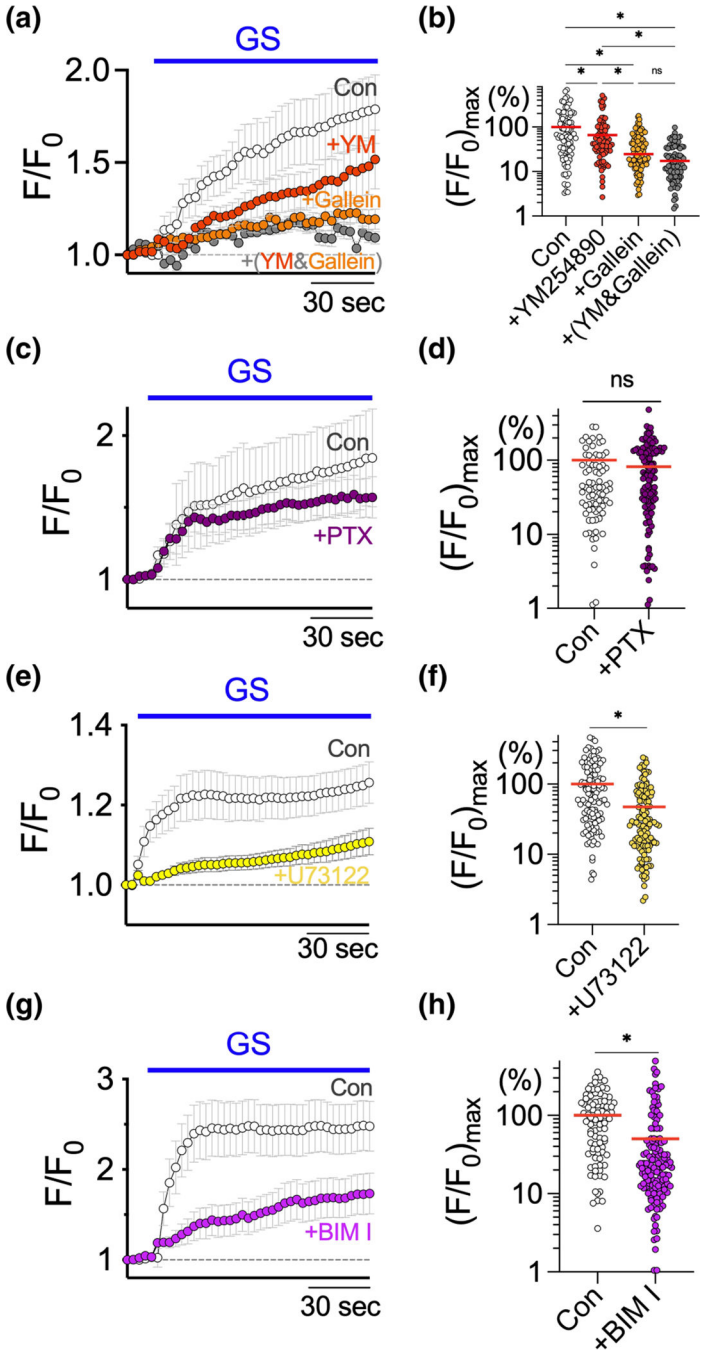

FIGURE 3.

GS utilizes various downstream signalling pathways in mouse sensory neurons. (a) 100 μM GS-induced responses in control DRG neurons (n = 121 cells) were compared with groups pretreated with inhibitors such as 10 μM YM254890 (Gαq/11 inhibitor; n = 93 cells), 10 μM gallein (Gβγ complex inhibitor; n = 130 cells) and both 10 μM YM254890 and 10 μM gallein ('YM&Gallein'; n = 108 cells). (b) Comparison of maximum responses ($[F/F_0]_{max}$) of groups pretreated with inhibitors used in (a). (c) 100 μM GS-induced responses in control DRG neurons (n = 85 cells) were compared with a group pretreated with 250

ng/ml PTX (Gαi/o inhibitor; $n = 130$ cells). (d) Comparison of $(F/F_0)_{max}$ between control and PTX-treated group. (e) 100 μM GS-induced responses in control DRG neurons ($n = 126$ cells) were compared with a group pretreated with 10 μM U73122 (PLC inhibitor; $n = 130$ cells). (f) Comparison of $(F/F_0)_{max}$ between control and U73122-treated group. (g) 100 μM GS-induced responses in control DRG neurons ($n = 92$ cells) were compared with a group pretreated with 10 nM BIM I (PKC inhibitor; $n = 142$ cells). (h) Comparison of $(F/F_0)_{max}$ between control and BIM I-treated group. Red horizontal bar indicates the average value of each group. $*P < 0.05$; ns, not significant

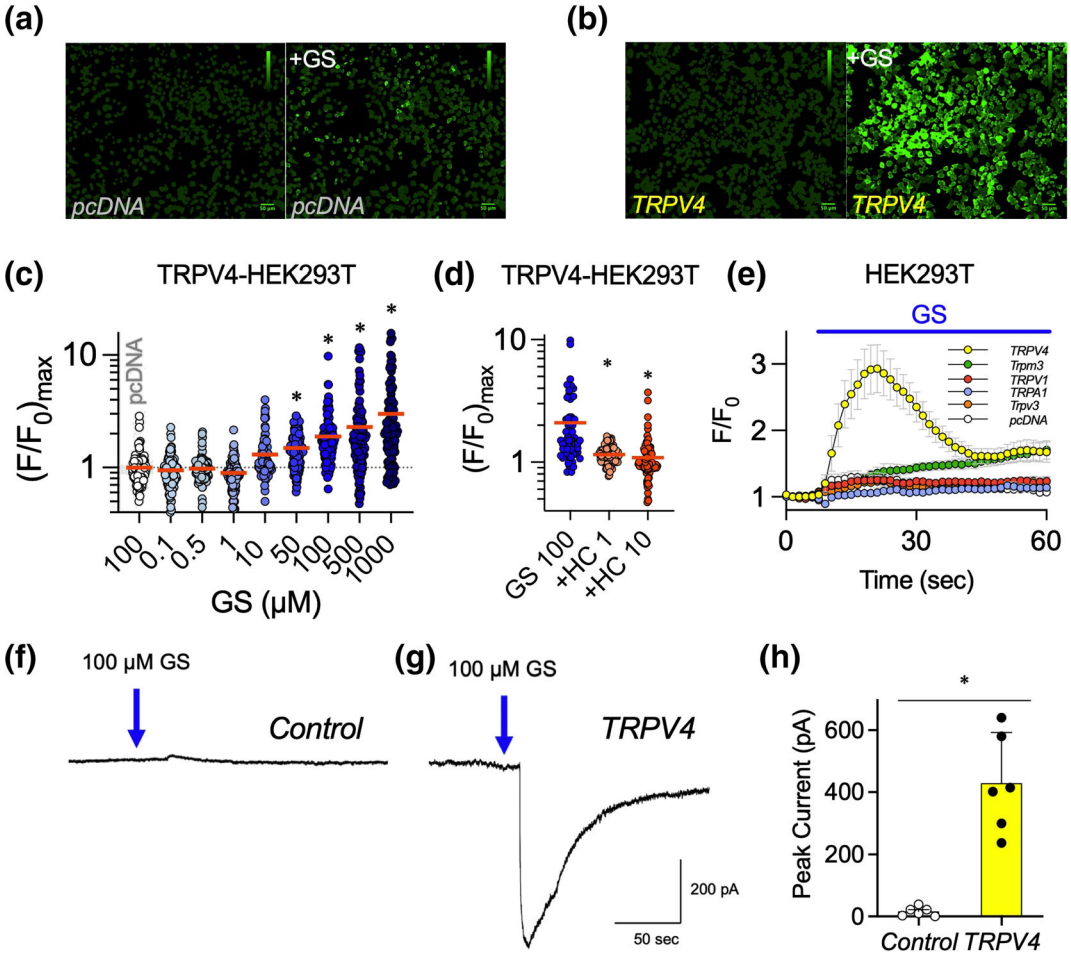

FIGURE 4.

GS can directly activate TRPV4. Representative calcium imaging results before and after 100 μM GS treatment upon HEK293T cells transiently expressing either mock vector (*pcDNA*; a) or *TRPV4* cDNA (b). (c) Summary of dose-dependent intracellular calcium responses induced by GS in HEK293T cells expressing TRPV4 ('TRPV4-HEK293T'). A total of 100 μM GS was treated on pcDNA-transfected group (n = 110 cells). Various concentrations of GS were applied on TRPV4-expressing groups (GS in μM: 0.1 [n = 109 cells], 0.5 [n = 112 cells], 1 [n = 108 cells], 10 [n = 82 cells], 50 [n = 127 cells], 100 [n = 134 cells], 500 [n = 122 cells] and 1,000 [n = 120 cells]). Red horizontal bar indicates the average value of each group. (d) A TRPV4-specific inhibitor HC067047 (1 μM [n = 118 cells] and 10 μM [n = 89 cells]) significantly inhibited the GS-induced calcium influx in the TRPV4-HEK293T compared to control ('GS 100', n = 62 cells). Red horizontal bar indicates the average value of each group. (e) Comparison of 50 μM GS responses in HEK293T cells transfected with either *pcDNA* (n = 160 cells), *TRPV1* (n = 170 cells), *Trpv3* (n = 127 cells), *TRPA1* (n = 139 cells), *Trpm3* (n = 149 cells) or *TRPV4* (n = 188 cells). Notice the significantly higher maximum response in TRPV4 than in others. (f–h) A whole-cell patch clamp experiment was performed in HEK293T cells transfected with either pIRES-eFGP-TRPV4 (TRPV4) or mock vector (control). The holding potential was −80 mV. (f) Cells transfected with a mock vector did not show any inward currents to the GS

treatment. (g) An inward current was observed in cells expressing TRPV4. (h) Summary of the peak inward currents between control versus TRPV4-expressing cells ($n = 6$ per group). *$P < 0.05$

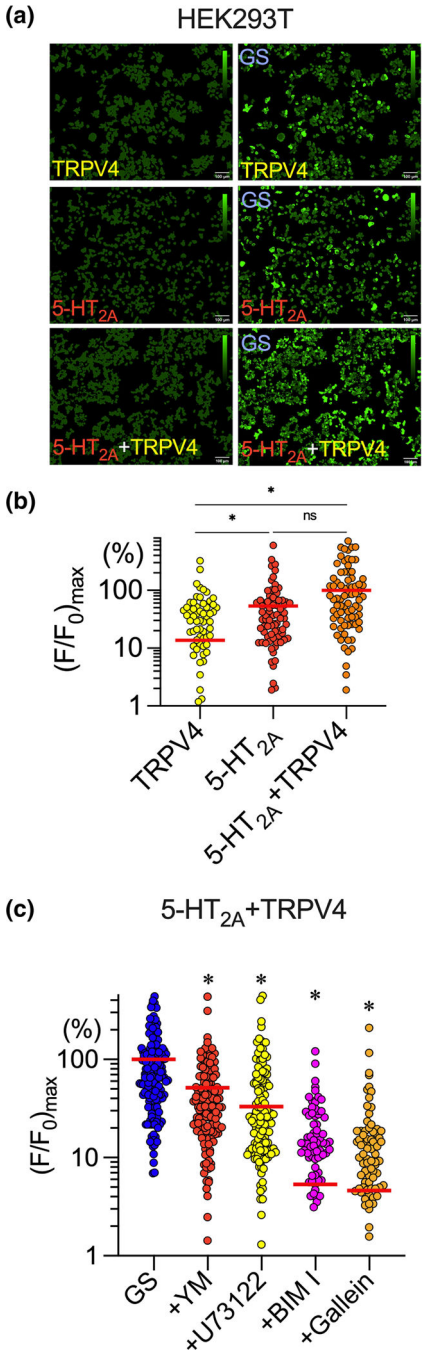

FIGURE 5.

Coexpression of both 5-HT_{2A} receptor and TRPV4 induces a stronger intracellular calcium influx. (a) Representative calcium imaging results before and after 25 μM GS treatment in cells expressing either TRPV4 (top row), 5-HT_{2A} receptor (5-HT_{2A}) (middle row) or both 5-HT_{2A} and TRPV4 ('5-HT_{2A} + TRPV4', bottom row). (b) Comparison of maximum responses ($[F/F_0]_{max}$) among TRPV4 (n = 108 cells), 5-HT_{2A} (n = 107 cells) and '5-HT_{2A} + TRPV4' (n = 110 cells) groups. (c) Maximum values of F/F_0 evoked by 25 μM GS (n = 186 cells) compared to pretreatment of inhibitors including 10 μM YM254890 (n = 177 cells), 10

μM U73122 (n = 174 cells), 10 nM BIM I (n = 146 cells) and 10 μM gallein (n = 182 cells) in '5-HT_{2A} + TRPV4'. Red horizontal bar indicates the average value of each group. *P < 0.05; ns, not significant

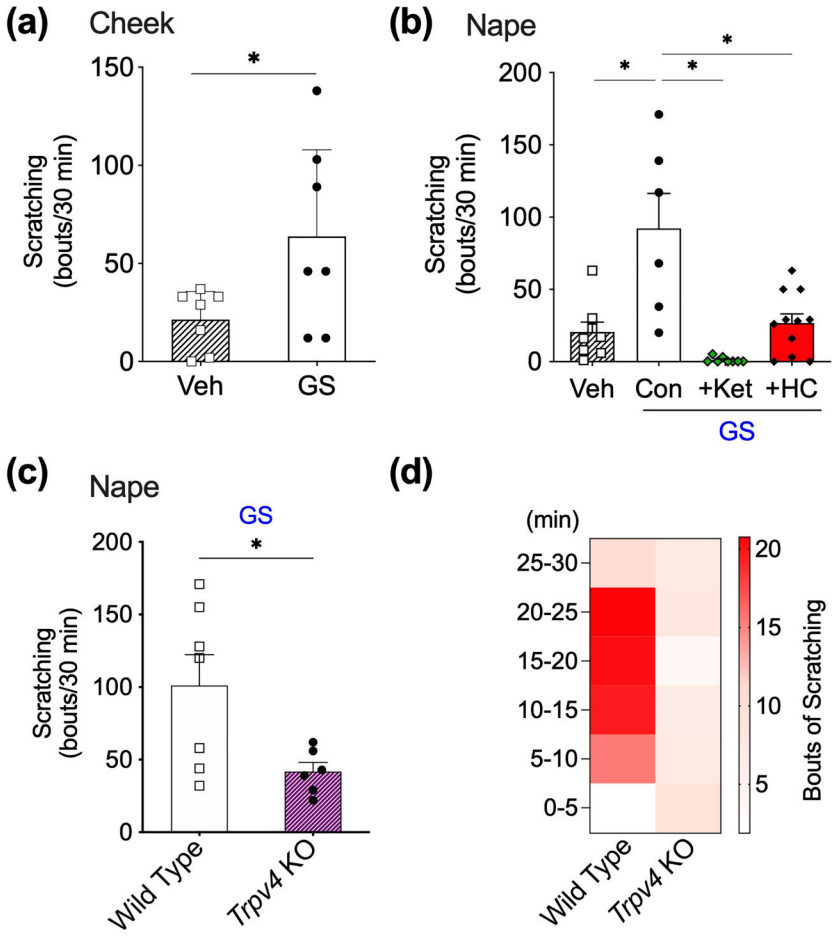

FIGURE 6.

GS evokes scratching behaviour via 5-HT_{2A} receptor and TRPV4 in mouse. (a) GS injection (250 nmol/site) in the cheek evoked scratching behaviours in ICR mice ('GS', $n = 7$) when compared to vehicle-injected group ('Veh', $n = 7$). (b) GS injection (250 nmol/site) in the nape elicited scratching behaviour in ICR mice ('Con', $n = 6$) compared to vehicle injection ('Veh', $n = 8$), which was significantly inhibited by pretreatment of 5-HT_{2A} receptor antagonist ketanserin ('+Ket', 3 mg/kg, $n = 8$) and TRPV4 antagonist HC067047 ('+HC', 10 mg/kg, $n = 11$). Bouts of scratching were counted for 30 min. (c) Bouts of scratching behaviour (30 min) evoked by 250 nmol/site GS were reduced in *Trpv4* KO mice ($n = 6$) than C57BL/6 wild-type mice ('WT', $n = 7$). (d) Heat map representation of scratching bouts of WT and *Trpv4* KO mice. Bouts of scratching are shown in colour for each 5-min interval. $*P < 0.05$

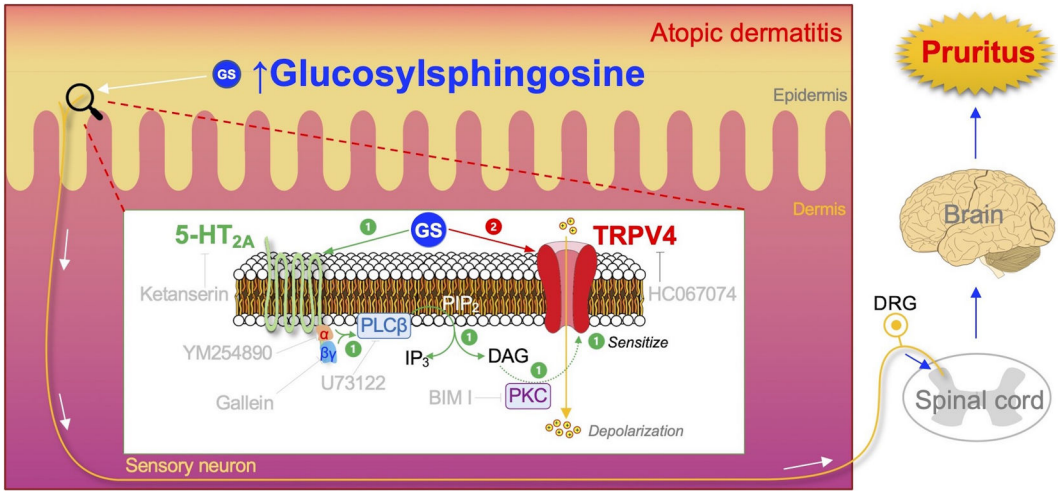

FIGURE 7.

A proposed signalling pathway for GS-evoked pruritus. The highly accumulated GS in the epidermis of patients with AD will activate the peripheral sensory neuron to induce pruritus in the following way: (1) GS activates 5-HT_{2A} receptor (5-HT_{2A}) with subsequent stimulation of PLC via Gαq/11 and Gβγ complex, which in turn breaks down phosphatidylinositol 4,5-bisphosphate (PIP_2) into inositol triphosphate (IP_3) and diacylglycerol (DAG). DAG will then activate phosphokinase C (PKC), which leads to sensitization of TRPV4. (2) Activation of the sensitized TRPV4 can be directly facilitated by GS, which will allow a massive influx of cations from the extracellular regions, increasing a chance to induce depolarization and possibly an action potential. This GS-induced electrical signal produced in the peripheral sensory neuron will be further transmitted through the spinal cord and to the brain, where the signal can finally be perceived as pruritus